ISSN 1070-3632, Russian Journal of General Chemistry, 2014, Vol. 84, No. 1, pp. 143–156. © Pleiades Publishing, Ltd., 2014.

Spectroscopic and Thermal Investigations of Transition and Non-Transition Metal Complexes of Penicillin G as Potential Biological Active Species[1]

Moamen S. Refat[a,b] and Foziah A. Al-Saif[c]

[a] *Department of Chemistry, Faculty of Science, Port Said, Port Said University, Egypt*
e-mail: msrefat@yahoo.com

[b] *Department of Chemistry, Faculty of Science, Taif University, 888 Taif, Kingdom Saudi Arabia*

[c] *Department of Chemistry, Faculty of Science, Princess Nora Bint Abdul Rahman University, Riyadh, Kingdom Saudi Arabia*

Received October 7, 2013

Abstract—Seven types of complexes were obtained when penicillin G potassium (pin) was reacted with transition and non-transition metal ions in methanol/distilled water mixed solvent. Magnetic susceptibilities and ESR spectra (Cu^{II} complex) of powdered samples indicated that the monomeric form of the complexes in the solid state, and the paramagnetic nature of the Cu^{II}, Ni^{II}, Mn^{II}, Cr^{III}, Co^{II}, and Fe^{III} complexes is attributable to the octahedral ligitional behavior of the potassium G penicillinate ligand. The antibacterial activity of the metal complexes were tested against some kind of bacteria and fungi strains and compared with penicillin G potassium activity. The possible mechanism of antibacterial action is discussed.

DOI: 10.1134/S1070363214010228

INTRODUCTION

Penicillin G potassium (Fig. 1) chelating agent has two carbonyl groups (–C=O) one of them for amide and the other for β-lactam ring. The penicillins have a widely broad-spectrum activity toward both Gram-positive and Gram-negative bacteria [1]. The presence of metal ions binded to parent drug play an important role in the modification of the proper structures of these antibiotics to push the antibacterial, antiviral, and antineoplastic activities [2–4]. Potential of the metal beta-lactam derivatives as antibiotic drugs were focused in line with application of bio-coordination chemistry [5–8]. There are limited solid and solution studies were reported in the literature for penicillin derivatives interacted with metal ions [9–19]. This paper is a continuation of our research [20–23] in the field of complexation between the transition and non-transition metals with commonly used pharmaceutical compounds. These results encouraged us to discuss the coordination chemistry of antibiotics with some transition and non-transition metal ions in an attempt to examine the modes of binding in the solid state and to study ibiological activity.

EXPERIMENTAL

All chemicals were of commercial origin and used without further purification. Penicillin G potassium (pin) and metal salts were received from BDH and Aldrich Companies.

Synthesis of penicillin G potassium (pin) complexes *(general procedure)*. Aqueous solutions of Penicillin G potassium (pin) ligand (2.0 mmol; 0.746 g) in 25 mL distilled water and 25 mL of methanol and 1.0 mmol of $MnCl_2 \cdot 4H_2O$ (0.198 g) were mixed and refluxed with stirring at 60°C for 30 min. The colored solid precipitated on cooling was filtered off, washed several times with water and little amount of methanol. Fe, Cr and Au complexes were prepared similarly, but with molar ratio of 1 : 3 (metal : pin) from $FeCl_3 \cdot 6H_2O$

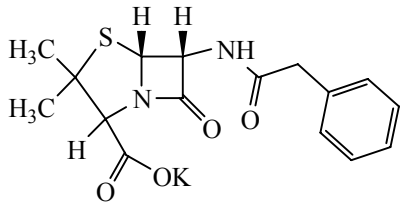

Fig. 1. Penicillin G potassium (pin) ligand.

[1] The text was submitted by the authors in English.

Table 1. Analytical and physical data for penicillin G potassium and its metal complexes

Complex (M_W, g/mol)	Color	Λm (Ω^{-1} cm^{-1} mol^{-1})	Elemental analysis (%) [found (calculated)		mp, °C
			C	H	
pin (372.48)	White	15	51.55	4.56	216
$[Cd(pin)_2]\cdot H_2O$ (**I**) (797.20)	White	23	47.98 (48.21)	4.32 (4.55)	>250
$[Zn(pin)_2]\cdot 2H_2O$ (**II**) (768.20)	White	26	49.86 (50.03)	4.87 (4.99)	<250
$[Ni(pin)_2]\cdot 3H_2O$ (**III**) (779.50)	Light Green	21	49.02 (49.31)	5.03 (5.17)	<250
$[Sr(pin)(H_2O)_2(Cl)]$ (**IV**) (492.50)	White	34	38.91 (39.02)	4.12 (4.30)	<250
$[Fe(pin)_2(Cl)(H_2O)]\cdot H_2O$ (**V**) (794.10)	Yellow	36	48.12 (48.40)	4.76 (4.82)	<250
$[Pt(pin)(Cl)_3]$ (**VI**) (634.82)	Yellow	46	30.14 (30.27)	2.64 (2.70)	<250
$[Au(pin)_2]\cdot Cl\cdot 3H_2O$ (**VII**) (953.23)	Brown	65	40.25 (40.32)	4.20 (4.23)	<250
[Pd(pin)(Cl)] (**VIII**) (475.26)	Brown	38	40.33 (40.44)	3.55 (3.61)	<250
$[Mg(pin)(H_2O)_2(Cl)]$ (**IX**) (429.20)	White	29	44.39 (44.78)	4.89 (4.93)	<250
$[Ca(pin)(H_2O)_2(Cl)]\cdot H_2O$ (**X**) (462.96)	White	35	41.32 (41.51)	4.84 (5.01)	<250
$[Ba(pin)(H_2O)_2(Cl)]\cdot H_2O$ (**XI**) (560.21)	White	36	34.09 (34.30)	3.96 (4.14)	<250
[Sn(pin)(Cl)] (**XII**) (487.55)	White	40	39.27 (39.42)	3.43 (3.51)	<250
$[Pb(pin)_2]\cdot 3H_2O$ (**XIII**) (928.01)	White	22	41.37 (41.42)	4.29 (4.34)	<250
$[Co(pin)(NO_3)(H_2O)]\cdot 2H_2O$ (**XIV**) (508.37)	Red	29	37.64 (37.80)	4.47 (4.56)	<250
$[Cr(pin)_2]\cdot Cl\cdot H_2O$ (**XV**) (772.23)	Violet	62	49.39 (49.77)	4.61 (4.70)	<250
$[Mn(pin)_2]\cdot H_2O$ (**XVI**) (739.72)	Buff	24	51.44 (51.96)	4.74 (4.91)	<250
$[Cu(pin)_2]\cdot H_2O$ (**XVII**) (748.33)	Dark green	22	51.08 (51.36)	4.80 (4.85)	<250

(0.270 g), $CrCl_3\cdot 6H_2O$ (0.267 g) or $NaAuCl_4\cdot xH_2O$ (0.40 g), respectively. The resulting penicillin G complexes were dried under vacuum over anhydrous calcium chloride. The analytical data for the obtained complexes are listed in Table 1.

Measurements. The elemental analyses (carbon and hydrogen contents) were performed by the microanalysis unit at Cairo University, Egypt, using a Perkin Elmer CHN 2400 instrument. The molar conductivities of freshly prepared 1.0×10^{-3} mol/cm^3 DMSO solutions were measured using Jenway 4010 conductivity meter. Electronic absorption spectra were recorded in DMSO within 900–200 nm range using an UV2 Unicam UV-Vis spectrophotometer, fitted with a quartz cell of 1.0 cm path length in Mansoura University. Infrared spectra in KBr discs were recorded on a Bruker FT-IR spectrophotometer (4000–400 cm^{-1}). Solid reflectance spectra were measured on UV-3101 PC, Shimadzu, UV-Vis NIR Scanning Spectrophotometer. Magnetic data were calculated using Magnetic Susceptibility Balance, Sherwood Scientific, at 25°C in Cairo University. The ^{1}H NMR spectra were recorded on a Varian Mercury VX-300 NMR spectrometer, using DMSO-d_6 as a solvent with TMS as an internal standard. The electron spin resonance (ESR) spectrum for copper(II) penicillin G complex was recorded on Jeol JES-FE2XG ESR-spectrometer equipped with Jeol microwave unit at 9.44 GHz. The thermal studies (TG/DTG) were carried out on a Shimadzu thermogravimetric analyzer under nitrogen flow. Scanning electron microscopy (SEM) images were taken on Quanta FEG 250 instrument. X-ray diffraction patterns for the selected penicillin G complexes were recorded on a X'Pert PRO PAN analytical X-ray powder diffraction instrument.

Antimicrobial activity assay. The antimicrobial activity of target penicillin G potassium and its complexes was evaluated by the standard disc diffusion technique [24, 25]. Procedure: Target organisms were inoculated in melted (at 50°C) trypticase soy agar + 0.6 % yeast extract medium [26]. Mold strains were inoculated in melted (at 50°C)

potato dextrose agar medium with heavy inoculums [26]. Then the inoculated medium were poured over a solid layer of uninoculated agar medium in sterilized Petri-dishes and left to solidify at 4°C (surface layer should be constant in volume and horizontally homogenous). Discs of Whatman No. 1 filter paper (6.0 mm in diameter) were sterilized by autoclaving at 121°C for 15 min. An accurate portion of each crystalline compound (dissolved in DMSO, 100 mg/mL) was aseptically added to each disc and left to dry. Each disc was aseptically placed on the middle of agar surface (in triplicate) and left at 4°C for 1 h, then plates were incubated. Gentamicin for bacterial strains and nystatin for fungal strains (10 μg/disc) were used as positive reference standards. The antimicrobial activity of target compounds was evaluated by measuring the average inhibition zone diameter (mm) against the test microorganisms.

Determination of the minimum inhibitory concentration (MIC). The MICs of each target compound against the tested bacterial strains were determined by tube dilution method [27] using Trypticase soy broth + 0.6% yeast extract [26, 28] Inoculated suspensions of the microorganisms were prepared from 12 h cultures. Each tested compound was dissolved in 10% DMSO and series of two fold dilutions, ranging from 10 to 200 μg/mL, were prepared in sterilized tubes. The MIC was defined as the lowest concentration of compound which the microorganism did not demonstrate visible growth (visible turbidity) and expressed as μg/mL.

Statistical analysis. Each of the measurements described was carried out in three replicate experiments and the results are recorded as mean ± standard deviation. The significantly different calculated at level of $p \leq 0.05$.

RESULTS AND DISCUSSION

The reaction of penicillin G potassium with a variety of di- and trivalent metal ions, gave slow-to-rapid deposition of microcrystalline solids, and despite numerous attempts, we have been unable to produce crystals suitable for X-ray structural analysis. However, the variable colours, melting points, conductivity data and element content (C and H) of these complexes indicate that they have a seven types of coordination modes: $[M(pin)_2]\cdot nH_2O$ (M = Cu^{II}, Cd^{II}, Zn^{II}, Ni^{II}, Pb^{II} or Mn^{II}; n = 1–3), $[M(pin)(H_2O)_2(Cl)]\cdot nH_2O$ (M = Sr^{II}, Mg^{II}, Ca^{II} or Ba^{II}; n = 0–1), $[M(pin)_2]Cl\cdot nH_2O$ (M = Au^{III} or Cr^{III}; n = 1–3), $[Pt(pin)(Cl)_3]$ (**VI**), [M(pin)Cl] (Pd^{II} or Sn^{II}), $[Co(pin)(NO_3)(H_2O)]\cdot 2H_2O$ (**XIV**) and $[Fe(pin)_2(Cl)(H_2O)]\cdot H_2O$ (**V**). These complexes are insoluble in water and in most organic solvents but soluble in DMSO. All pin complexes have melting points higher than parent antibiotic.

Conductivity measurements. The conductance values of the resulted complexes are listed in Table 1. The conductivity of penicillin G complexes was measured in DMSO at room temperature. All the complexes have the conductance values for 10^{-3} mol/cm^3 solutions in the range of 15 to 65 Ω^{-1} cm^2 mol^{-1}. It is suggesting that penicillin G complexes have three types of conductance nature [29, 30]: (*i*) electrolyte nature for Au^{III} and Cr^{III} complexes according to the presence of one chloride ion outside the coordination sphere, (*ii*) slightly electrolyte nature for Sr^{II}, Mg^{II}, Ca^{II}, Ba^{II}, Pt^{IV}, Pd^{II}, Sn^{II}, Fe^{III}, and Co^{II} complexes due to the sharing of anion (chloride or nitrate ion) in the chelation process, also, the difference in the values of molar conductance between these complexes is due to the number of coordinated anions), and (*iii*) non electrolyte nature for Cu^{II}, Cd^{II}, Ni^{II}, Mn^{II}, Zn^{II}, and Pb^{II} complexes which have a lower conductance values (Table 1) comparing with the parent penicillin G potassium. The presence of chloride ions in penicillin G complexes (inside or outside coordination sphere) with the exception for Cu^{II}, Cd^{II}, Ni^{II}, Mn^{II} and Zn^{II} complexes was detected by the addition of few drops of concentrated silver nitrate/HNO_3 reagent leading to the appearance of white precipitate (AgCl).

Infrared and Raman spectra. The main IR frequencies observed for penicillin G potassium and its complexes can be seen in Table 2. The Infrared spectroscopy is the most reliable technique of interpretive the exhibit of distinguish groups, all the synthesized complexes were discussed spectroscopically in the mid infrared region 4000-400 cm^{-1}, as all the complexes contain aromatic, β-lactam, carboxylate, amido and dimethyl thiazolidine groups. The C–H aromatic stretching vibrations occur between 3000–3100 cm^{-1} [31]. The prominent bands in the spectra of pin complexes appear in the low frequencies range between 950–650 cm^{-1} assigned to out-of-plane bending of the ring C–H bonds. The in-plane bending bands exist in the 1300–1000 cm^{-1} range. The characteristic C=C skeletal stretching vibrations lead to a group of bands within 1650–1450 cm^{-1} region [32]. The infrared spectrum of penicillin G potassium showed absorptions at 3079 cm^{-1} due to C–H aromatic, 3368 cm^{-1} for NH amide, 1775 cm^{-1} due to C=O of β-

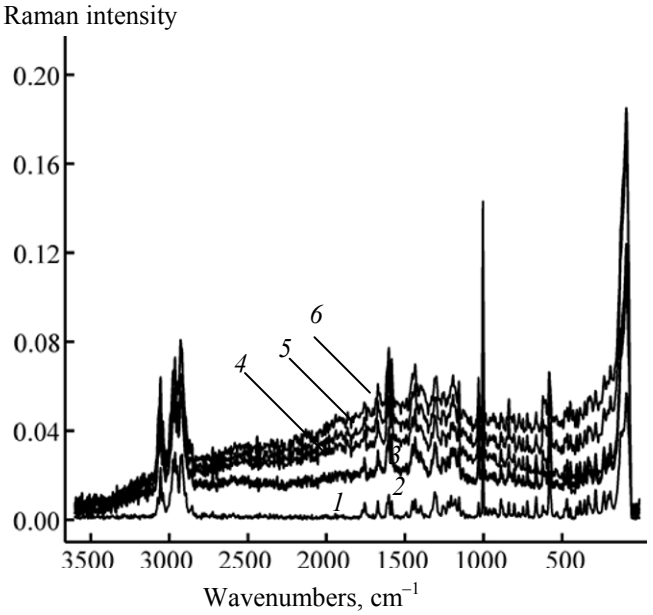

Fig. 2. Raman spectra of complexes: (*1*) pin, (*2*) **X**, (*3*) **XIV**, (*4*) **V**, (*5*) **XII**, and (*6*) **II**.

lactam, 1671 cm^{-1} of C=O for carboxylate group, 1612 cm^{-1} assigned to asymmetric stretching vibration of COO carboxylate group and 1393 cm^{-1} due to symmetric stretching vibration of COO carboxylate group. In comparison between pin ligand and its Cu^{II}, Cd^{II}, Ni^{II}, Pb^{II}, Mn^{II}, Sr^{II}, Mg^{II}, Ca^{II}, Ba^{II}, Au^{III}, Cr^{III}, Pt^{IV}, Pd^{II}, Sn^{II}, Co^{II}, Zn^{II}, and Fe^{III} complexes, there are informative changes in frequencies and intensiveness, corresponding to complexity situation between metal ions mentioned above and penicillin G potassium. The pin complexes can be classified into two ways of chelating, the first coordination mode concerning Cu^{II}, Cd^{II}, Ni^{II}, Mn^{II}, Sr^{II}, Mg^{II}, Ca^{II}, Ba^{II}, Au^{III}, Cr^{III}, Pt^{IV}, Pd^{II}, Sn^{II}, and Co^{II} ions towards pin ligand show the distinguish infrared bands at 1752–1728 cm^{-1} due to ν(C=O); β-lactam which shifted toward lower frequencies and also at 1672–1634 cm^{-1} of ν(C=O) amide group, suggesting that chelation of ligand occurs via oxygen atoms of both carbonyl groups of β-lactam and amide groups. The second way of coordination process in case of Fe^{III}, Pb^{II}, and Zn^{II} ions have prominent bands at 1778 cm^{-1} due to ν(C=O) of β-lactam and 1644–1649 cm^{-1} of ν(C=O) amide group, suggesting that the ν(C=O) of β-lactam ring does not coordinate to metal ions. The stretching vibrations of both carbonyl groups (β-lactam and amide groups) partially or completely overlapped with the $\nu_{as}(COO)$ asymmetric stretching vibration mode. The carboxylate group is able to coordinate to metal ions by different modes (Scheme 1) [33].

Scheme 1. Coordination modes of the carboxylate group

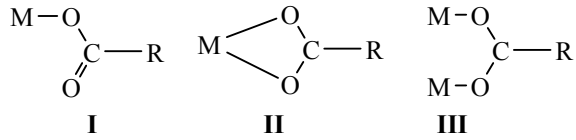

(1) When the carboxylate group coordinaes toward metal ion as a monodentate chelate, the difference wavenumbers between the asymmetric and symmetric stretching vibrations of carboxylate groups [$\Delta\nu = \nu_{as}(COO^-) - \nu_s(COO^-)$] is larger than 200 cm^{-1}. (2) When Δν is considerably smaller than 200 cm^{-1}, the carboxylate group acts as bidentate chelatant [34]. (3) The characteristic wavenumber difference, Δν, is larger than that for chelated ions and nearly the same as observed for ionic compounds. Based on the above results, it was possible to distinguish the coordination mode of the $-COO^-$ group. The pin ligand exhibit two absorption bands detectable around 1612 and 1393 cm^{-1} for the $\nu_{as}(COO^-)$ and $\nu_s(COO^-)$, respectively. In the infrared spectra of the synthesized complexes, the band of carboxylate was substantially shifted to lower wavenumbers or disappeared. The difference value ($\nu_{as} - \nu_s$) for the COO^- groups and the shift of these bands, by comparison with the data for sodium salt, may suggest that bidentate chelating and bridging COO^- groups [35]. When the difference values ($\nu_{as} - \nu_s$) of the COO^- groups are higher or nearly similar comparable with potassium salt, it suggested that the carboxylate groups act as monodentate chelatant. The hydrated complexes $[M(pin)_2]\cdot nH_2O$ (M = Cu^{II}, Cd^{II}, Zn^{II}, Ni^{II}, Pb^{II} or Mn^{II}; n = 1–3), $[M(pin)(H_2O)_2(Cl)]\cdot nH_2O$ (M = Sr^{II}, Mg^{II}, Ca^{II} or Ba^{II}; n = 0–1), $[M(pin)_2]Cl\cdot nH_2O$ (M = Au^{III} or Cr^{III}; n = 1–3), $[Co(pin)(NO_3)(H_2O)]\cdot 2H_2O$ and $[Fe(pin)_2(Cl)(H_2O)]\cdot H_2O$, have a broad or shoulder absorption band of ν(O–H) of the water molecule with maximum above 3400 cm^{-1}.

In case of $[Co(pin)(NO_3)(H_2O)]\cdot 2H_2O$ complex, the characteristic stretching vibrations of the bidentate nitrate group, NO_3^-, is observed at 1384 and 1030 cm^{-1} attributed to $\nu_{as}(NO_2)$ and $\nu_s(NO_2)$, respectively [35, 36]. The stretching motion of [ν(N=O)] is observed at 1435 cm^{-1} as a weak band, while the two bending motion of the type $\delta(NO_2)$ are well resolved and observed at 784 and 661cm^{-1} as a weak bands. The assignments of the other three different ν(M–O) [oxygen's of ν(C=O); β-lactam, ν(C=O) amide group,

Table 2. Assignments of the infrared spectral bands (cm^{-1}) for penicillin *G* potassium and its metal complexes

Compound	Assignments					
	ν(N–H)	ν(C=O) β-lactam	ν(C=O) amide	ν_{as}(COO)	ν_{s}(COO)	Δν
pin	3368	1775	1671	1612	1393	219
I	3303	1743	1649	1586	1395	191
II	3377	1778	–	1647	1375	272
III	3391	1743	1653	1520	1281	239
IV	3389	–	–	1599	1399	200
V	3340	1778	1649	1533	1318	215
VI	3144	1749	1672	1403	1200	203
VII	3145	–	1661	1520	1284	236
VIII	3141	1752	–	1646	1403	243
IX	3391	–	–	1623	1404	219
X	3387	–	–	1603	1403	200
XI	3380	–	–	1593	1393	200
XII	3376	1733	–	1644	1391	253
XIII	3308	1731	1644	1563	1383	180
XIV	3376	1744	1655	1517	1287	230
XV	3393	1738	1645	1500	1276	224
XVI	3392	–	–	1604	1394	210
XVII	3253	1728	1634	1456	1261	195

carboxylate group] vibrations in penicillin G complexes are observed in the range 400–600 cm^{-1} [37, 38]. It is noteworthy to refer to a Raman spectra technique (Fig. 2) in order to identify spectral bands due to metal-pin vibration modes, but unfortunately, there are many bands overlapping to each other than infrared spectral technique [39]. On examining of the Raman spectra of the penicillin G complexes, it was found that the spectra of Ca^{II} and Sn^{II} complexes are more pronounced making it easy to compare with the parent ligand. Raman spectra of $[Ca(pin)(H_2O)_2(Cl)]\cdot H_2O$ and [Sn(pin)(Cl)] complexes show the bands at (513, 489, 457, 428, 407, and 374 cm^{-1}) and (519, 498, 479, 457, 428, and 351 cm^{-1}), respectively, due to M–O vibration motions of pin as a tridentate ligand via oxygen atom of carbonyl group of both β-lactam and amide groups as well as oxygen atom of carboxylate group coordinated in a monodentate mode.

Electronic spectra and magnetic measurements. Tables 3 and 4 refer to the electronic (UV-vis and solid reflectance) spectra and magnetic measurements assignments which are important and interesting items for most chemical characterizations to obtain important information about the structural features of the complexes. Penicillin G potassium free ligand, which is a vital antibiotic drug, has a distinguish absorption bands in two regions: 275–255 nm and 330–320 nm due to intraligand excitation [39]. Upon complexation with some transition metal ions (Ni^{II}, Fe^{III}, Pt^{IV}, Au^{III}, Pd^{II}, Co^{II}, Cr^{III}, Mn^{II}, and Cu^{II}), due to interaction with the metal ion there is an interesting change in the electronic properties of the system. New bands in the visible region due to d-d absorption and charge transfer spectra from metal to ligand (M–L) or ligand to metal (L–M) can be observed and this data can be processed to obtain information regarding the structure and geometry of the complexes [40]. UV-visible peaks corresponding to the π→π* transitions in the penicillin G complexes were observed at 276, 296, 272, 272, 270, 274, 284, 264 and 280 nm for the Ni^{II}, Fe^{III}, Pt^{IV}, Au^{III}, Pd^{II}, Co^{II}, Cr^{III}, Mn^{II}, and Cu^{II} complexes, respectively [41]. The peaks belonging to *n*→π* transitions are recorded at wavelengths (312 and 332 nm), 324 nm, (292 and 320 nm), (294 and 318 nm), 336 nm, (294, 318 and 348 nm), 382 nm, 375 nm, (328

Table 3. Electronic spectral bands (nm) and magnetic moments of the selected penicillin G complexes[a]

Complex	Transition, λ, nm			μ_{eff}, BM	*n*	Hybrid orbitals	Spin-only, BM	Stereochemistry
	π→π*	*n*→π*	LMCT					
pin	275–255	330–320	–	–	–	–	–	–
III	276	312 332	418	2.49	2	sp^3d^2	2.83	Octahedral
V	296	324	405 490	2.35	1	d^2sp^3	1.73	Octahedral
VI	272	272 320	352 364 394	–	–	–	–	Four coordinated
VII	272	294 318	364 398	–	–	–	–	Six coordinated
VIII	270	336	380	–	–	–	–	Four coordinated
XIV	274	294 318 348	364 386 512	1.78	1	d^2sp^3	1.73	Octahedral
XV	284	382	420 552	2.52	2	d^2sp^3	2.83	Octahedral
XVI	264	375	405	2.15	1	d^2sp^3	1.73	Octahedral
XVII	280	328 382	432 635	1.52	1	sp^3d^2	1.73	Octahedral

[a] (*n*) – unparid electrons.

and 382 nm), respectively, for Ni^{II}, Fe^{III}, Pt^{IV}, Au^{III}, Pd^{II}, Co^{II}, Cr^{III}, Mn^{II}, and Cu^{II} complexes [42]. The first range can be assigned to π→π* transitions in the aromaticity of double bond while the second range is most probably due to the *n*→π* transitions of β-lactam, carboxylate, amido, and dimethyl thiazolidine groups. The third type of transition in visible region located at 418 nm, (405 and 490 nm), (352, 364, and 394 nm), (364 and 398 nm), 380 nm, (364, 386, and 512 nm), (420 and 552 nm), 405 nm, and (432 and 635 nm), respectively, and can be assigned to the ligand-to-metal charge transfer bands LMCT from the electronic lone pairs of respective oxygen's to the metal ions [43]. The detectable weak-to-strong intensity bands within the three types of transitions in the free pin ligand were changed in the spectra of the metal complexes.

Table 4. Solid reflectance spectral bands (cm^{-1}) and assignments of the penicillin *G* complexes

Comp. no.	Spectral data, cm^{-1}	Electronic transition	Assignments
III	14814 20161	$^3A_{2g}(F) \rightarrow {}^3T_{1g}(F)$ $^3A_{2g}(F) \rightarrow {}^3T_{1g}(P)$	Distorted octahedral
V	16260 19157	$^6A_1 \rightarrow {}^4A_1, {}^4E(G)$ $^6A_1 \rightarrow {}^4T_2(G)$	Distorted octahedral
XIV	12674 15748 18484	$^4T_{1g}(F) \rightarrow {}^4T_{2g}(F)$ $^4T_{1g}(F) \rightarrow {}^4A_{2g}(F)$ $^4T_{1g}(F) \rightarrow {}^4T_{2g}(P)$	Distorted octahedral
XV	17668 23753 33898	$^4A_{2g} \rightarrow {}^4T_{2g}(F)$ $^4A_{2g} \rightarrow {}^4T_{1g}(F)$ $^4A_{2g} \rightarrow {}^4T_{1g}(P)$	Distorted octahedral
XVI	17544 18382 20408	$^6A_{1g} \rightarrow {}^4T_{1g}(G)$ $^6A_{1g} \rightarrow {}^4T_{2g}(G)$ $^6A_{1g} \rightarrow {}^4E_g(G), {}^4A_{1g}(G)$	
XVII	16474 21097	$^2B_{1g} \rightarrow {}^2E_g$ $^2B_{1g} \rightarrow {}^2B_{2g}$	

Magnetic properties. The effective magnetic moment (μ_{eff}) of Mn^{II}, Fe^{III}, Ni^{II}, Cu^{II}, Co^{II} and Cr^{III} complexes give the spin only value $\{\mu_{s.o.} = [n(n+2)]^{1/2}$ BM$\}$ corresponding to the number of unpaired electron. The variation from the spin only value is attributed to the orbital contribution and it varies with the nature of coordination and consequent delocalize-

tion. A mononuclear complex of Manganese(II) of the formula $[Mn(pin)_2]H_2O$ that Mn(II) is in the +2 oxidation state, the complex is expected to have magnetic moment of 2.18 BM with number of unparid electrons (n = 1) corresponding to d^5 configuration and the experimental value is 2.15 BM in a good agreement with expected value. The ferrum(III) pin complex has a 2.35 BM magnetic moment with configuration d^5 octahedral stereochemistry, hybrid orbital d^2sp^3, one unpaired electrons (n = 1), spin only equal 1.73 BM and expected magnetic moment is 2.25 BM The experimental value of μ_{eff} of Fe^{III} complex is 2.35 B.M that closely matches expected value. The magnetic moment, configurations, stereochemistry, hybrid orbitals, number of unpaired electrons, spin-only and expected magnetic values of Ni^{II}, Cu^{II}, Co^{II}, and Cr^{III} pin complexes are (2.49 BM, d^8, octahedral, sp^3d^2, n = 2, 2.83 and 3.32 BM), (1.52 BM, d^9, octahedral, sp^3d^2, n = 1, 1.73 and 1.96 BM), (1.78 BM, d^7, octahedral, d^2sp^3, n = 1, 1.73 and 1.88 BM), and (2.52 BM, d^4, octahedral, d^2sp^3, n = 2, 2.83 and 3.27 BM), respectively. The lower magnetic value of $[Ni(pin)_2]$, $[Cu(pin)_2]\cdot H_2O$, $[Co(pin)(NO_3)(H_2O)]\cdot 2H_2O$, and $[Cr(pin)_2]\cdot Cl\cdot H_2O$ complexes assigned to that individual magnetic moments are aligned in opposite directions so that they superimpose each other. Thus the value of magnetic moment of a complex would give valuable insights into its constitution and structure. The magnetic susceptibility measurements thus help to predict the possible geometry of the metal complexes [44]. The data for diffuse solid reflectance spectra of the penicillin G complexes listed in the Table 4. The observed spectra of Mn^{II}, Fe^{III}, Ni^{II}, Cu^{II}, Co^{II}, and Cr^{III} pin complexes agreed with the distorted octahedral geometry. The spectrum of Mn^{II} complex shows three medium -to-weak intensity bands at 17544, 18382 and 20408 cm^{-1}, which can be assigned to $^6A_{1g} \rightarrow {}^4T_{1g}(G)$, $^6A_{1g} \rightarrow {}^4T_{2g}(G)$, and $^6A_{1g} \rightarrow {}^4E_g(G)$, $^4A_{1g}(G)$, respectively, for an Mn^{II} ion in case of distorted octahedral field [43]. The electronic spectrum of the octahedral Fe^{III} complex showed two distinguish bands. The band at 16260 cm^{-1} may be assigned to the $^6A_1 \rightarrow {}^4A_1$, $^4E(G)$ transition and the other at 19157 cm^{-1} to $^6A_1 \rightarrow {}^4T_2(G)$ [45]. The reflectance spectrum of the Ni^{II} complex showed two identified bands at 14814 and 20161 cm^{-1}, assigned to the transitions $^3A_{2g}(F) \rightarrow {}^3T_{1g}(F)$ and, $^3A_{2g}(F) \rightarrow {}^3T_{1g}(P)$ respectively [44]. The spectrum of the Ni^{II} complex suggests an octahedral geometry. The diffuse reflectance spectrum of copper(II) complex showed two allowed transitions (16474 and 21097 cm^{-1}), namely $^2B_{1g} \rightarrow {}^2E_g$ and $^2B_{1g} \rightarrow {}^2B_{2g}$. These bands suggested distorted octahedral geometry around Cu^{II} [43]. Consequently, the electronic spectrum of octahedral Co^{II} complex has three types of transitions at 12674, 15748, and 18484 cm^{-1} due to $^4T_{1g}(F) \rightarrow {}^4T_{2g}(F)$, $^4T_{1g}(F) \rightarrow {}^4A_{2g}(F)$,

Table 5. ESR spectral parameters of the complex **XVII**

Comp. no.	$g_{\|}$	$g_{\perp}$	g_{av}	$A_{\|}$, cm^{-1}	$A_{\perp}$, cm^{-1}	ΔB (G)	Assignments
XVII	1.7605	1.8581	1.8104	137	145	167	Distorted octahedral

Table 6. ^{1}H NMR spectral data of penicillin G potassium free ligand, **VI**, and **XI** complexes

Assignments, ppm	Complex		
	penicillin G potassium	**VI**	**XI**
6H, of dimethyl group of thiazolidine ring	1.459, 1.573	1.167–1.535	1.062–2.088
2H; CH_2 group	3.447	3.286	3.502
1H; thiazolidine ring	3.543	3.312	3.650
H; NH of amide group	3.859	3.371	3.750
2H; β-lactam	5.333	4.917	4.278
5H; benzene ring	7.276, 8.690	7.483, 8.257	7.261, 8.096

Table 7. XRD spectral data of **VII** and **XV** complexes

Complex	2θ, deg	d, Å	Relative intensity, %	Full width at half maximum (FWHM)	Particle size, nm
VII	22.997	3.8641	25.8		
	29.961	2.9799	6.50		
	32.661	2.7395	100[a]	0.2941	5
	40.285	2.2369	5.60		
	43.559	2.0761	3.10		
	46.887	1.9362	19.8		
	52.753	1.7339	5.50		
	58.266	1.5882	14.6		
	68.348	1.3713	3.50		
	73.152	1.2927	2.50		
	77.759	1.2272	4.30		
XV	28.362	3.1442	100[a]		
	40.540	2.2234	59.7		
	50.236	1.8147	16.9		
	66.385	1.4071	18.3		
	73.639	1.2854	8.50		

[a] The maximum diffraction patterns according to the highest value of intensity.

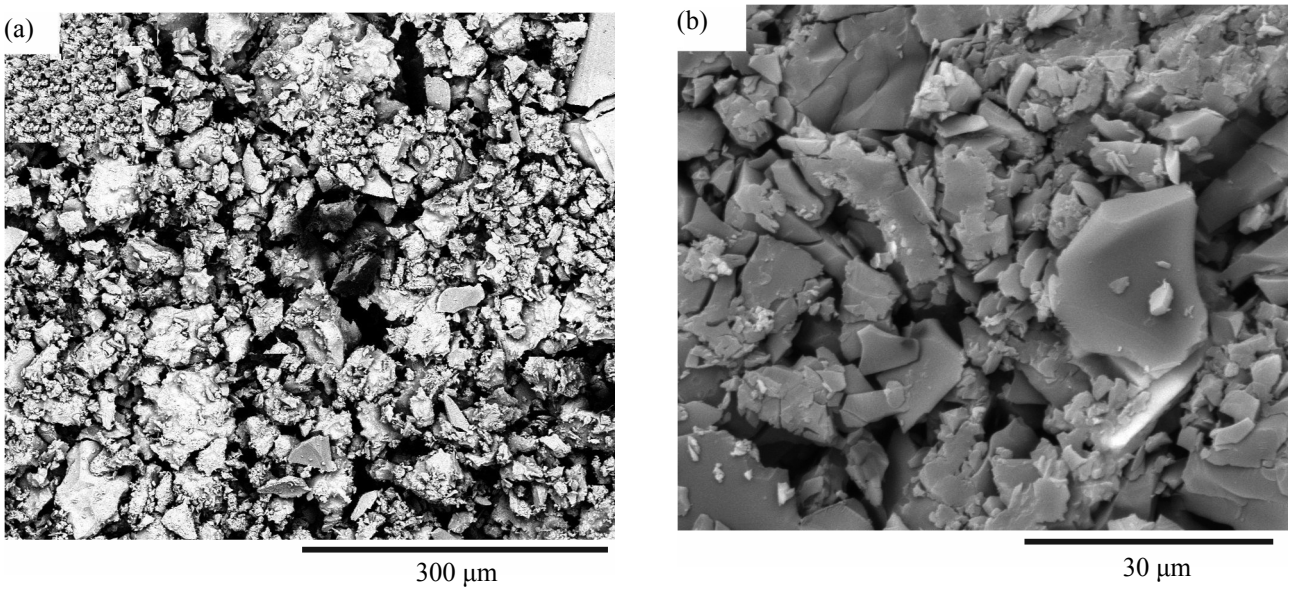

Fig. 3. SEM photo of (a) **VII** and (b) **XV** complexes.

$^4T_{1g}(F) \rightarrow {}^4T_{2g}(P)$ [46], respectively. Finally, the electronic spectrum of Cr^{III} complex exhibits three transitions at 17668, 23753, and 33898 cm^{-1} assignable to $^4A_{2g} \rightarrow {}^4T_{2g}(F)$, $^4A_{2g} \rightarrow {}^4T_{1g}(F)$, and $^4A_{2g} \rightarrow {}^4T_{1g}(P)$, respectively, which explain the octahedral geometry around the chromium atom [47, 48].

Electron spin resonance. The electron spin resonance technique is useful to identify the geometry and state of electrons in metal ion of the complexes field. Herein, the ESR spectrum of the Cu(II) complex was analyzed and the related parameters are given in Table 5. The solid-state ESR spectra of some of the complexes exhibit axially symmetric g-tensor parameters with that the copper site has a $d_{x^2-y^2}$ ground-state characteristic of tetrahedral, square-planar, or octahedral stereochemistry. The $g_\perp > g_\parallel$ for synthesized Cu(II) complex, $[Cu(pin)_2]\cdot H_2O$ (**XVII**), indicates a distorted octahedral geometry [49].

Proton nuclear magnetic resonance. The proton NMR peaks of penicillin G potassium free ligand, $[Pt(pin)(Cl)_3]$ and $[Ba(pin)(H_2O)_2(Cl)]\cdot H_2O$ complexes in DMSO-d_6 are listed in the Table 6. Protons of Penicillin G potassium free ligand (Scheme 2) were assigned as: δ, ppm: 1.459 (3H, of one methyl group of dimethyl thiazolidine ring), 1.573 (3H, of the other methyl group of dimethyl thiazolidine ring), 3.447 (2H; CH_2 group), 3.543 (1H; thiazolidine ring), 3.859 (H; NH of amide group), 5.333 (2H; β-lactam), 7.276 and 8.690 (5H; benzene ring). The $[Ba(pin)(H_2O)_2(Cl)]\cdot H_2O$ complex: δ(ppm) 1.062–2.088 (6H, of dimethyl group of thiazolidine ring), 3.502 (2H; CH_2 group), 3.650 (1H; thiazolidine ring), 3.750 (H; NH of amide group), 4.278 (2H; β-lactam), 7.261 and 8.096 (5H; benzene ring). Concerning $[Pt(pin)(Cl)_3]$ complex, δ, ppm: 1.167–1.535 (6H, of dimethyl group of thiazolidine ring), 3.286 (2H; CH_2 group), 3.312 (1H; thiazolidine ring), 3.371 (H; NH of amide group), 4.917 (2H; β-lactam), 7.483 and 8.257 (5H; benzene ring). The above results show that in both cases of Pt^{IV} and Ba^{II} complexes, all proton signals of benzene, β-lactam, amido, and dimethyl thiazolidine groups are downfield shifted in comparison with free penicillin G potassium ligand.

Scheme 2. Proton positions and chemical shifts (δ, ppm) of free penicillin G potassium ligand

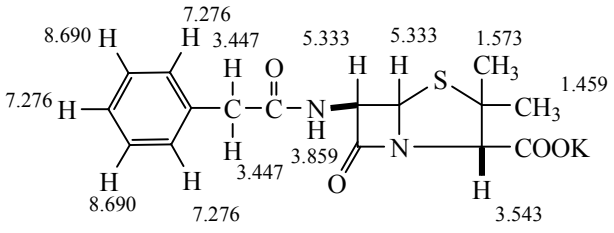

Scanning electron microscopy and X-ray powder diffraction. The microstructure, surface morphology and chemical composition of Cr^{III} and Au^{III} penicillin G complexes were studied using SEM. Typical scanning electron micrographs are shown in Figs. 3a, 3b. The surface morphology of SEM micrograph reveals

the well uniform nature of the complexes with variant grain sizes and shapes. Clear large grains are obtained with agglomerates for $[Cr(pin)_2]Cl{\cdot}H_2O$ (**XV**) and $[Au(pin)_2]Cl{\cdot}3H_2O$ (**VII**) complexes, Figs. 3a, 3b. The distribution of the grain size is inhomogeneous. X-ray powder diffraction patterns in the range of $4° < 2\theta < 80°$ of the **XV** and VII complexes were done. The definite diffraction data like angle (2θ, deg), interplanar spacing (*d* value, Å), and relative intensity (%) are summarized in Table 7. The X-ray patterns refer to the crystalline nature of penicillin G complexes. The variable diffractograms of Cr^{III} and Au^{III} complexes can be attributed to the formation of new structures. The values of 2θ, *d* value (the average volume of the crystal dimension normal to diffracting plane), full width at half maximum (FWHM) of prominent intensity peak, relative intensity (%) and particle size of complexes are compiled in Table 7. The maximum diffraction patterns of Cr^{III} and Au^{III} complexes exhibited at 2θ (*d* value, Å) = 28.362 (3.1442) and 32.661 (2.7395), respectively. The crystallite size could be estimated from XRD patterns by applying FWHM of the characteristic peaks using Deby–Scherrer equation (1) [50].

$$D = K\lambda/\beta\cos\theta, \quad (1)$$

where *D* is the particle size of the crystal gain, *K* is a constant (0.94 for Cu grid), λ is the X-ray wavelength (1.5406 Å), θ is the Bragg diffraction angle and β is the integral peak width. The particle size was estimated according to the highest value of intensity compared with the other peaks. These data gave an impression that the particle size located within nano scale range.

Thermal studies. Thermal behavior of penicillin G complexes was studied upon TG and DTG diagrams. The thermal decomposition data for all complexes are listed in Table 8. The thermal degradation process occurs in two-to-four various steps. According to the weight loss in each step, the following decomposition moieties may be proposed for Cu^{II}, Cd^{II}, Ni^{II}, Pb^{II}, Mn^{II}, Sr^{II}, Mg^{II}, Ca^{II}, Ba^{II}, Pt^{IV}, Zn^{II}, Pd^{II}, Sn^{II}, Co^{II}, Au^{III}, Cr^{III}, and Fe^{III} complexes All the penicillin G complexes are decompose progressively. The decomposition of hydrated complexes started by the release of water molecules which presented outside (uncoordinated) or inside (coordinated) coordination sphere at temperature range of 35–191°C with endothermic DTG peaks. The second-to-four decom-position steps are assigned to the initial decomposition of coordinated pin ligand.

$$\text{pin} \xrightarrow{220\text{–}600^\circ\text{C}} \uparrow\text{pin} + \text{potassium (metal)} + \text{residual carbon},$$

$$[Cd(pin)_2]{\cdot}H_2O \xrightarrow{40\text{–}130^\circ\text{C}} [Cd(pin)_2] + \uparrow H_2O,$$

$$[Cd(pin)_2] \xrightarrow{130\text{–}600^\circ\text{C}} \uparrow 2\text{pin} + CdO + \text{residual carbon},$$

$$[Zn(pin)_2]{\cdot}2H_2O \xrightarrow{50\text{–}138^\circ\text{C}} [Zn(pin)_2] + \uparrow 2H_2O,$$

$$[Zn(pin)_2] \xrightarrow{138\text{–}600^\circ\text{C}} \uparrow 2\text{pin} + ZnO,$$

$$[Ni(pin)_2]{\cdot}3H_2O \xrightarrow{50\text{–}125^\circ\text{C}} [Ni(pin)_2] + \uparrow 3H_2O,$$

$$[Ni(pin)_2] \xrightarrow{125\text{–}600^\circ\text{C}} \uparrow 2\text{pin} + NiO + \text{residual carbon},$$

$$[Sr(pin)(H_2O)_2(Cl)] \xrightarrow{151\text{–}234^\circ\text{C}} [Sr(pin)_2(Cl)] + \uparrow 2H_2O,$$

$$[Sr(pin)_2(Cl)] \xrightarrow{234\text{–}600^\circ\text{C}} \uparrow\text{pin} + \uparrow HCl + SrCO_3 + \text{residual carbon},$$

$$[Fe(pin)_2(H_2O)(Cl)]{\cdot}H_2O \xrightarrow{89\text{–}181^\circ\text{C}} [Fe(pin)_2(Cl)] + \uparrow 2H_2O,$$

$$[Fe(pin)_2(Cl)] \xrightarrow{181\text{–}600^\circ\text{C}} \uparrow 2\text{pin} + \uparrow HCl + FeO + \text{residual carbon},$$

$$[Pt(pin)(Cl)_3] \xrightarrow{200\text{–}600^\circ\text{C}} \uparrow\text{pin} + \uparrow 3HCl + PtO_2 + \text{residual carbon},$$

$$[Au(pin)_2]{\cdot}Cl{\cdot}3H_2O \xrightarrow{62\text{–}191^\circ\text{C}} [Au(pin)_2]{\cdot}Cl{\cdot}H_2O + \uparrow 2H_2O,$$

$$[Au(pin)_2]{\cdot}Cl{\cdot}H_2O \xrightarrow{191\text{–}600^\circ\text{C}} \uparrow 2\text{pin} + \uparrow HCl + \uparrow H_2O + Au + \text{residual carbon},$$

$$[Pd(pin)(Cl)] \xrightarrow{141\text{–}600^\circ\text{C}} \uparrow\text{pin} + \uparrow HCl + Pd\uparrow,$$

$$[Mg(pin)(H_2O)_2(Cl)] \xrightarrow{53\text{–}600^\circ\text{C}} \uparrow\text{pin} + \uparrow HCl + 2H_2O + MgSO_4 + \text{residual carbon},$$

$$[Ca(pin)(H_2O)_2(Cl)]{\cdot}H_2O \xrightarrow{41\text{–}109^\circ\text{C}} [Ca(pin)(H_2O)_2(Cl)] + \uparrow H_2O,$$

$$[Ca(pin)(H_2O)_2(Cl)] \xrightarrow{109\text{–}600^\circ\text{C}} \uparrow\text{pin} + \uparrow HCl + \uparrow 2H_2O + CaCO_3 + \text{residual carbon},$$

$$[Ba(pin)(H_2O)_2(Cl)]{\cdot}H_2O \xrightarrow{65\text{–}120^\circ\text{C}} [Ca(pin)(H_2O)_{1.5}(Cl)] + \uparrow 1.5H_2O,$$

$$(pin)(H_2O)_{1.5}(Cl)] \xrightarrow{120\text{–}600^\circ\text{C}} \uparrow\text{pin} + \uparrow HCl + \uparrow 1.5H_2O + BaCO_3 + \text{residual carbon},$$

$$Ba[Sn(pin)(Cl)] \xrightarrow{150\text{–}600^\circ\text{C}} \uparrow\text{pin} + \uparrow HCl + SnO + \text{residual carbon},$$

$$[Pb(pin)_2]{\cdot}3H_2O \xrightarrow{144\text{–}166^\circ\text{C}} [Pb(pin)_2] + \uparrow 3H_2O,$$

$$[Pb(pin)_2] \xrightarrow{166\text{–}600^\circ\text{C}} \uparrow 2\text{pin} + PbO + \text{residual carbon},$$

$$[Co(pin)(NO_3)(H_2O)]{\cdot}2H_2O \xrightarrow{79\text{–}131^\circ\text{C}} [Co(pin)(NO_3)(H_2O)] + \uparrow 2H_2O,$$

$$[Co(pin)(NO_3)(H_2O)] \xrightarrow{131–600°C} \uparrow pin + \uparrow NO_2 + \uparrow H_2O + CoO + \text{residual carbon},$$

$$[Cr(pin)_2]\cdot Cl\cdot H_2O \xrightarrow{61–600°C} \uparrow 2pin + \uparrow HCl + \uparrow H_2O + 1/2Cr_2O_3 + \text{residual carbon},$$

$$[Mn(pin)_2]\cdot H_2O \xrightarrow{35–100°C} [Mn(pin)_2] + \uparrow H_2O,$$

$$[Mn(pin)_2] \xrightarrow{100–600°C} \uparrow 2pin + MnSO_4 + \text{residual carbon},$$

$$[Cu(pin)_2]\cdot H_2O \xrightarrow{50–125°C} [Cu(pin)_2] + \uparrow H_2O,$$

$$[Cu(pin)_2] \xrightarrow{125–600°C} \uparrow 2pin + CuO + \text{residual carbon}.$$

Suggested structures. The different formulas of pin complexes can be classified upon type of metal ions as follows; $[M(pin)_2]\cdot nH_2O$ (where M = Cu^{II}, Cd^{II}, Zn^{II}, Ni^{II}, Pb^{II} or Mn^{II}; n = 1–3), $[M(pin)(H_2O)_2(Cl)]\cdot nH_2O$ (where M = Sr^{II}, Mg^{II}, Ca^{II} or Ba^{II}; n = 0–1), $[M(pin)_2]Cl\cdot nH_2O$ (where M = Au^{III} or Cr^{III}; n = 1–3), $[Pt(pin)(Cl)_3]$ (**VI**), [M(pin)Cl] (where M = Pd^{II} or Sn^{II}), $[Co(pin)(NO_3)(H_2O)]\cdot 2H_2O$ (**XIV**), and $[Fe(pin)_2(Cl)(H_2O)]\cdot H_2O$ (**V**). The configuration was that the penicillin G is coordinated with all metal ions through oxygen's of amide, β-lactam and carboxylate

Table 8. Thermogravimetric data of penicillin G potassium and its complexes

Complex	Tempature range, °C	DTG	Decomposed assignments		Total weight loss, %
			losses species	residual species	
pin	220–600	252, 341	pin	K (metal) Residual carbons	57.240
I	40–130 130–600	43 214	H_2O 2pin	CdO Residual carbons	66.340
II	50–138 138–600	75 222, 405	$2H_2O$ 2pin	ZnO	88.503
III	50–125 125–600	75 201, 507	$3H_2O$ 2pin	NiO Residual carbons	86.023
IV	151–234 234–600	153, 217 289, 585	$2H_2O$ HCl + pin	$SrCO_3$ Residual carbons	42.294
V	89–181 181–600	97 250	$2H_2O$ HCl + 2pin	FeO Residual carbons	81.577
VI	200–600	212	3HCl + pin	PtO_2 Residual carbons	22.737
VII	62–191 191–600	125 301	$2H_2O$ 2pin + HCl + H_2O	Au (metal) Residual carbons	73.226
VIII	141–409 409–600	320 511	pin + HCl + Pd	Residual carbons	98.233
IX	53–600	71, 277, 432	pin + HCl + $2H_2O$	$MgSO_4$ Residual carbons	26.088
X	41–109 109–600	75 219, 288, 397	pin + HCl + $2H_2O$	$CaCO_3$ Residual carbons	53.517
XI	65–120 120–600	89 209, 282, 500	$1.5H_2O$ $1.5H_2O$ + HCl + pin	$BaCO_3$ Residual carbons	45.935
XII	150–600	231, 570	pin + HCl	SnO Residual carbons	37.954
XIII	144–166 166–600	153 208, 273	$3H_2O$ 2pin	PbO Residual carbons	45.028
XIV	79–131 131–600	96 266, 432	$2H_2O$ H_2O + NO_2 + pin	CoO Residual carbons	66.694
XV	61–600	266, 396, 547	pin + HCl + H_2O	$½Cr_2O_3$ Residual carbons	81.903
XVI	35–100 100–600	55 269, 345, 476	H_2O 2pin	$MnSO_4$ Residual carbons	64.829
XVII	50–125 125–600	73 145, 234, 575	H_2O 2pin	CuO Residual carbons	72.418

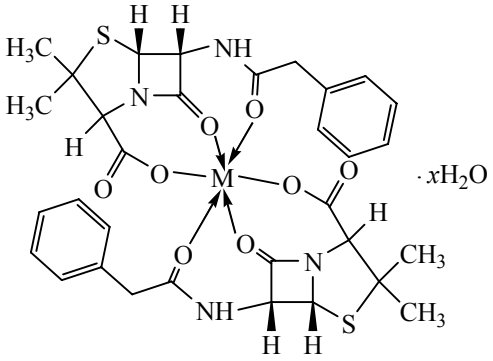

$[M(pin)_2]\cdot nH_2O$ (M = Cu^{II}, Cd^{II}, Ni^{II}, or Mn^{II}; n = 1–3).

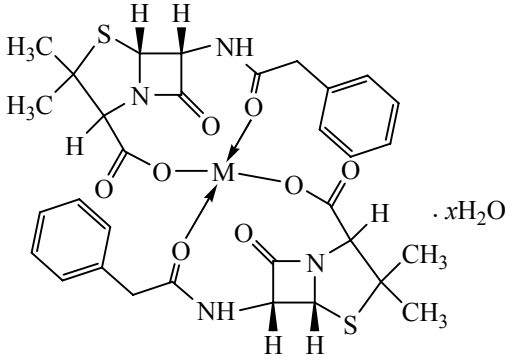

$[M(pin)_2]\cdot nH_2O$ (M = Zn^{II} or Pb^{II}; n = 2–3).

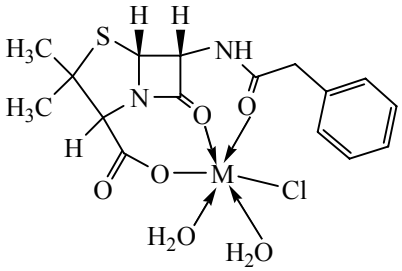

$[M(pin)(H_2O)_2(Cl)]\cdot nH_2O$

(M = Sr^{II}, Mg^{II}, Ca^{II} or Ba^{II}; n = 0–1).

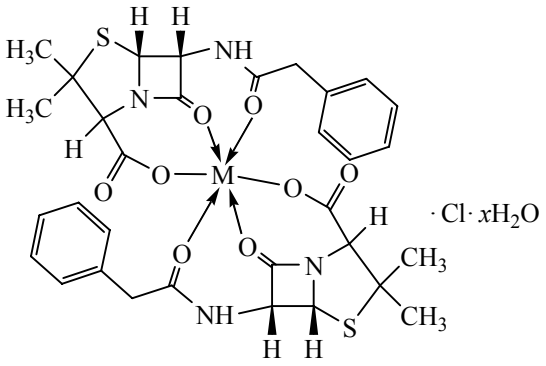

$[M(pin)_2]Cl\cdot nH_2O$ (M = Au^{III} or Cr^{III}; n = 1–3).

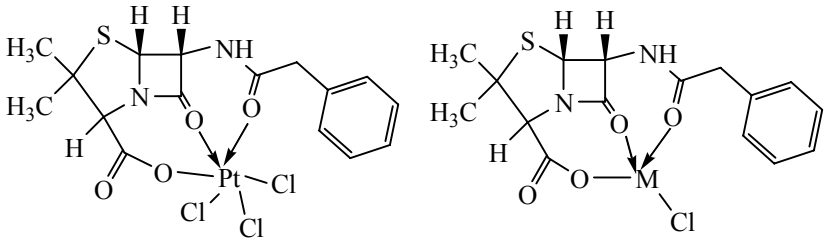

$[M(pin)Cl]$ (M = Pd^{II} or Sn^{II}).

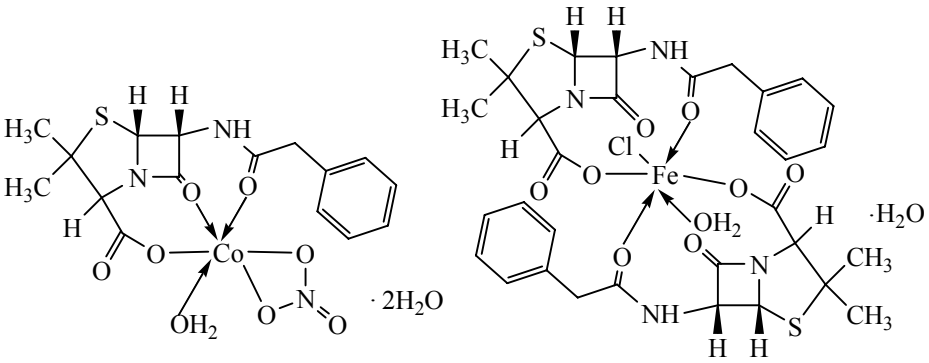

Fig. 4. Suggested chelating of penicillin G complexes towards respective metal ions.

Table 9. Species; strains and cultivation conditions of used microorganism[a]

Species of microorganisms	Strains	Cultivation conditions
Gram-positive bacteria		
G+ bacilli, spore-forming	Bacillus subtilis[b]	TSA + YE, 30°C for 24 h
G+ cocci	Staphylococcus aureus (ATCC 29213)	TSA + YE, 37°C for 24 h
Gram-negative bacteria		
G– short rods	Escherichia coli (ATCC 25922)	TSA + YE, 37°C for 24 h
G– short rods	Salmonella typhimurium (ATCC 19430)	TSA + YE, 37°C for 24 h
Yeast	Saccharomyces cerevisia[b]	TSA + YE, 30°C for 48 h
Mold	Fusarium oxysporum[c]	PDA, 25°C for 72 h
Mold	Rhizoctonia solani[c]	PDA, 25°C for 72 h

[a] G+: Gram-positive bacteria, G-: Gram-negative bacteria, TSA+YE: Trypticase Soy Agar + 0.6% Yeast Extract, PDA: Potato Dextrose Agar.
[b] Obtained from Department of Microbiology, Agriculture faculty, Cairo University.
[c] Obtained from Plant pathology Institute, Agricultural Research Center, Egypt.

Table 10. The Minimum Inhibitory Concentration (MIC) μg/mL ; mean ±SD values of penicillin G potassium parent drug and some selected complexes against affected strains

Compound	*Staphylococcus aureus*	*Bacillus subtilis*	*Escherichia coli*	*Salmonella typhimurium*
pin (parent drug)	15.1 ±1.7	19.3 ± 2.5	_	87.9 ± 3.7
Cd^{II}	43.1 ± 2.6	32.1 ± 1.9	_	_
Ca^{II}	18.3 ±1.5	35.2 ± 1.1	63.1 ± 3.4	37.8 ± 2.1
Cu^{II}	16.6 ± 2.1	20.7 ± 3.1	_	_
Pb^{II}	25.1 ± 1.9	38.1 ± 2.1	_	_
Mn^{II}	27.3 ± 2.3	30.4 ± 3.0	_	_
Fe^{III}	30.3 ± 1.4	33.1 ± 1.5	_	_
Mg^{II}	_	_	_	_
Co^{II}	20.1 ± 2.5	38.3 ± 1.9	_	_
Ba^{II}	36.1 ± 2.2	47.6 ± 2.4	_	_
Sn^{II}	19.4 ±1.2	23.1 ± 1.7	82.5 ± 4.1	76.8 ± 3.6

groups, while the Zn^{II}, Pb^{II} and Fe^{III} ions coordinated with penicillin G via both oxygen atoms of amide and carboxylate groups. Therefore, from the results presented in this paper the metal complexes have four-to-six coordination numbers, as can be seen in Fig. 4.

Antimicrobial studies. Antimicrobial activity of a number of obtained complexes was observed by agar disc diffusion technique against Gram positive (*Bacillus subtilis* and *Staphylococcus aureus*) and Gram negative (*Escherichia coli* and *Salmonella typhimurium*) bacteria, yeast (*Saccharomyces cerevisia*) and two strains of mold (*Fusarium oxysporu* and *Rhizoctonia solani*). Results from the agar disc diffusion tests indicated that penicillin G complexes (except for Mg^{II}complex) displayed a variable degree

of antibacterial activity against Gram positive strains and Ca^{II} complex **X** has some antibacterial activity against Gram negative strains compared with parent drug (Table 9). The highest inhibition zone and lowest concentration to be effective against bacterial strains (MIC values as presented in Table 10) of penicillin derivatives was against *Staphylococcus aureus* in order of: $Cu^{II} > Sn^{II} > Fe^{III} > Pb^{II} > Mn^{II}$. The result indicated that the substituent of metal cation from parent drug with another metals (transition or non-transition) influence the effectiveness of penicillin derivatives as antibacterial agents. The possible mechanism of the action of penicillin complexes in the present study can be explained on the basis of cell permeability, the lipid membrane around the cell tend to penetration of lipid-soluble materials; liposolubility is an important factor that controls the antimicrobial activity. The polarity of the different ion will be reduced due to overlap of ligand orbital and partial sharing of the positive charge of the metal ion with donor groups [51]. It is likely that the increased liposolubility of the ligand upon metal complexation may contribute to its facile transport into the bacterial cell which blocks the metal binding sites in enzymes of microorganisms [52]. The variety of antibacterial activity and kind of bacteria, may be due to the differences in the susceptibility of the test organisms to different penicillin complexes, this could be attributed to a variation in the rate of the penetration through the cell wall and cell membrane structures [53].

ACKNOWLEDGMENTS

This work was supported by grants from Princess Nora Bint Abdul Rahman University, Riyadh, Saudi Arabia under project Grants No. 22/32. On the other hand, we express our gratitude to Dr. Mahmoud A. Mohamed, Taif University, for his efforts being made in biological studies.

REFERENCES

1. Holten, K.B. and Onusko, E.M., *American Family Physician*, 2000, vol. 62(3), p. 611.
2. Chaires, J.B. and Waring, M.J., *Met Enzymol.*, San Diego, CA: Academic Press, vol. 340, 2001.
3. Tullius, T.D., *Metal-DNA Chemistry*, ACS Symposium Series 402, the American Chemical Society, 1989.
4. Umezawa, H., Maeda, K., Takeuchi, T., and Okami, Y., *J. Antibiot*., 1966, vol. 19, p. 200.
5. Anacona, J.R. and Silva, G.D., *J. Chilean Chem. Soc*., 2010, vol. 50, no. 2, p. 447.
6. Anacona, J.R. and Toledo, C., *Trans. Met. Chem*., 2001, vol. 26, p. 228.
7. Anacona, J.R. and Alvarez, P., *Trans. Met. Chem*., 2002, vol. 27, p. 856.
8. Anacona, J.R. and Rodriguez, I., *J. Coord. Chem*., 2004, vol. 57, p. 1263.
9. Weiss, A., Fallab, S. and Erlenmeyer, H., *Helv. Chim. Acta*, 1957, vol. 40, no. 3, p. 611.
10. Cressman, W.A. and Niebergall, P.J., *J. Pharm. Pharmacol.*, 1967, vol. 19, no. 11, p. 774.
11. Harwood, R.J., Niebergall, P.J., Sugita, E.T., and Schnaare, R.L., *J. Pharm. Sci.*, 1972, vol. 61, no. 1, p. 82.
12. Gensmantel, N.P., Proctor, P., and Page, M.I., *J. Chem. Soc. Perkin Trans.*, 1980, vol. 2, no. 11, p. 1725.
13. Hay, R.W., Basak, A.K., and Pujari, M.P., *J. Chem. Soc. Dalton. Trans.*, 1989, vol. 2, p. 197.
14. Fazakerley, G.V., Jackson, G.E., and Linder, P.W., *J. Inorg. Nucl. Chem.*, 1976, vol. 38, no. 7, p. 1397.
15. Van Crimpen, P. C., Van Bennekom, W.P., and Bult, A., *Pharm. Weekblad Sci. Ed.*, 1988, vol. 10, no. 6, p. 259.
16. Hernandez Martinez, J., Martinez, P.J., Gutierrez, P., and Martinez, M.I., *Talanta*, 1992, vol. 39, no. 6, p. 637.
17. Gutierrez Navarro, P., Hernandez Blazquez, I., and Quintero Osso, et al., B. *Int. J. Biol. Macromol.*, 2003, vol. 33, nos. 4–5, p. 159.
18. Grochowski, T. and Samochocka, K., *Polyhedron*, 1991, vol. 10, no. 13, p. 1473.
19. Anacona, J. and Figueroa, R.E.M., *J. Coord. Chem*., 1999, vol. 48, no. 2, p.181.
20. Refat, M.S. and El–Metwaly, N.M., *J. Mol Str*., 2011, vol. 988, nos. 1–3, p. 111.
21. Refat, M.S. and Mohamed, S.F., *Spectrochimica Acta A*, 2011, vol. 82, p. 108.
22. Refat, M.S., *J. Mol. Str*., 2010, vol. 969, p. 163.
23. Refat, M.S. and El-Shazly, S.A., *Eur. J. Med. Chem*., 2010, vol. 45, no. 7, p. 3070.
24. Gillies, R.R., *Dodds. Bacteriology Illustrated*, 5 ed., Churchill Livingstone, Edinburgh, London Melbourne and New York, 1984, pp. 160–165.
25. Ingolfsdottir, K., Hajalmarsdottir, M.A., Sigurdsson, A., Gudjonsdottir, G.A., Bryonjolfsdottir, A., and Steingreimsson, O.A., *Agents and Chemotherapy Antimicrob*., 1997, vol. 4, p. 215.
26. APHA. *Standard Methods for the Examination of Dairy Products*, 17 ed., Am. Publ. Health Assoc. Inc., Washington DC, 1978.
27. Sokmen, A., Gulluce, M., Akpulat, H.A., Daferera, D., Tepe, B., and Polissiou, M., *Food Cont*., 2004, vol. 15, no. 8, p. 627.
28. Evans, W.C. and Trease, *Evan*'s *Pharmacognosy*, 14 ed., WB Saunders, London, 1996, p. 780.

29. Geary, W.J., *Coord. Chem. Rev*., 1971, vol. 7, p. 81.
30. Refat, M.S., *Spectrochimica Acta Part A*, 2007, vol. 68, p. 1393.
31. Pavia, D.L., Lampman, G.M., and Kriz, G.S., *Introduction to Spectroscopy*, 3 ed., Brooks Cole USA, 2000, p. 515.
32. Chakrawarti, B.P., Srivastava, B., and Vijayvargiya, B.L., *J. Ind. Chem. Soc*., 1993, vol. 70, p. 158.
33. Deacon, G.B. and Phillips, R.J., *Coord. Chem. Rev*., 1980, vol. 33, p. 227.
34. Alcock, N.W., Culver, J., and Roe, S.M., *J. Chem. Soc. Dalton Trans*., 1992, p. 1447.
35. Nakamoto, K., *Infrared and Raman Spectra of Inorganic and Coordination Compounds*, New York: Wiley, 1997.
36. Ross, S.D., *Inorganic Infrared and Raman Spectra*, London : Mc Graw Hill, 1972.
37. Beattie, I.R., Gilson, T.R., and Ozin, G.A., *J. Chem. Soc. (A),* 1969, p. 534.
38. Nakagawa, I. and Shimanouchi, T., *Spectrochim. Acta Part A*, 1964, vol. 20, p. 429.
39. Anacona, J.R. and Acosta, F., *J. Coord. Chem*., 2006, vol. 59, p. 621.
40. Singh, H.L. and Vershney, A.K., *Bioinorg. Chem. Appl*., 2006, p. 1**.**
41. Ozturk, O.F., Sekerci, M., and Ozdemir, E., *Russ. J. Coord. Chem*., 2005, vol. 31, p. 687.
42. Ozturk, O.F., Sekerci, M., and Ozdemir, E., *Russ. J. Gen. Chem*., 2006, vol. 76, p. 36.
43. Allan, J.R., Baird, N.D., and Kassyk, A.L., *J. Therm. Anal*., 1979, vol. 16, p. 79.
44. Lever, A.B.P., *Coord. Chem. Rev*., 1968, vol. 3, p. 119.
45. Bailar, J.C., Emeleus, H., Nyholm, J.R., and Dickenson, A.F., *Comprehensive Inorganic Chemistry*, Pergamon Press, 1975, vol. 3, p. 517.
46. Mondal, N., Dey, D.K., Mitra, S., and Abdul Malik, K.M., *Polyhedron*, 2000, vol. 19, p. 2707.
47. Lee, D.L., *New Concise in Inorganic Chemistry*, New York: ELBS, 1991.
48. Dubey, R.K., Dubey, U.K., and Mishra, C.M., *Indian J. Chem*., 2007, vol. 47A, p. 1208.
49. Cozar, O., David, L., Chis, V., Damian, G., Todica, M., and Agut, C., *J. Mol. Str*., 2001, vols. 563–564, p. 371.
50. Quan, C.X., Bin, L.H., and Bang, G.G., *Mater. Chem. Phys*., 2005, vol. 91, p. 317
51. Tumer, M., Koksal, H., and Sener, M.K., *Trans. Met. Chem*., 1999, vol. 24, p. 414
52. Muhammad, I., Javed, I., Shahid, I., and Nazia, I., *Turk. J. Biol*., 2007, vol. 31, p. 67
53. Cox, S.D., Mann, C.M., Markham, J.L., Gustafson, J.E., Warmington, J.R., and Wyllie, S.G., *Molecules*, 2001, vol. 6, no. 1, p. 87